

Anchor Layout Optimization for Ultrasonic Indoor Positioning Using Swarm Intelligence

Daan Delabie*, Thomas Wilding[§], Liesbet Van der Perre*, Lieven De Strycker*

*KU Leuven, WaveCore, Department of Electrical Engineering (ESAT), KU Leuven Ghent, 9000 Ghent, Belgium

[§]Graz University of Technology, Austria

daan.delabie@kuleuven.be

Abstract—Indoor positioning applications are craving for ever higher precision and accuracy across the entire coverage zone. Optimal anchor placement and the deployment of multiple distributed anchor nodes could have a major impact in this regard. This paper examines the influences of these two difficult to approach hypotheses by means of a straightforward ultrasonic 3D indoor positioning system deployed in a real-life scenario via a geometric based simulation framework. To obtain an optimal anchor placement, a particle swarm optimization (PSO) algorithm is introduced and consequently performed for setups ranging from 4 to 10 anchors. In this way, besides the optimal anchor placement layout, the influence of deploying several distributed anchor nodes is investigated. In order to theoretically compare the optimization progress, a system model and Cramér-Rao lower bound (CRLB) are established and the results are quantified based on the simulation data. With limited anchors, the placement is crucial to obtain a high precision high reliability (HPHR) indoor positioning system (IPS), while the addition of anchors, to a lesser extent, gives a supplementary improvement.

Index Terms—Localization, Particle swarm optimization, Simulation, Ultrasonic applications, Acoustics, Cramer Rao bounds

I. INTRODUCTION

IPSs are aiming at an ever higher accuracy and reliability over the entire space of interest to enable applications such as object tracking in industry, hospitals, retail shops and venues. To obtain HPHR systems it is important, in addition to using better algorithms, to also scrutinize the anchor placement layout to which often none or little attention is paid. However, a thoughtful anchor placement layout dedicated to a given space can significantly increase accuracy and reliability [1].

Typically there is not one optimal anchor placement layout that optimizes HPHR properties for all target positions, but there are several possibilities that show similar results [2]. Optimal anchor placement is mostly conducted for area-based localization [3], [4]. To the best of our knowledge, optimal 3D anchor placement layout exploration has so far not been carried out, except in [5], focusing on a minimum dilution of precision (DOP) value for a certain number of beacons. In addition, the deployment of more distributed anchor nodes can increase spatial diversity, creating more redundancy to overcome reverberation and non-line-of-sight (NLoS) effects [1]. It is clear that in complex rooms with many obstacles, additional anchor nodes are desired. Typically, the more anchor nodes the better the accuracy, which is proven by measure-

ments [6], [7] and simulations [7]–[9]. Mostly CRLBs are determined followed by a quest for the most closely related possible configurations via brute force searching or in an incremental way [2]. Other researchers use methods such as genetic algorithms (GAs) [1] or swarm intelligence (SI) algorithms [8], [9] to search for a viable solution.

Both the anchor placement puzzle and the desired amount of deployable anchors are difficult questions to solve. In this work we propose an optimization method based on SI, namely particle swarm optimization (PSO), whereby an optimal anchor placement layout in a practical 3D space is suggested for different numbers of anchors. The elaborated optimization method uses the variance of the 3D Euclidean distance error as a metric for the cost function. We strive for an optimal scenario in which the positioning accuracy is distributed as uniformly as possible over the entire room. Depending on the application, the optimal scenario can be defined differently, resulting in another optimization metric, e.g. the P95 value. For the positioning itself, a room simulation model [10] taking into account reverberation and directivities is used in which ultrasonic chirps are exploited for time of flight (ToF) measurements. The accuracy for 270 different locations in the room is determined in order to get the positioning in the entire room as reliable and accurate as possible.

To provide a clear picture of the proposed methods, the ultrasonic IPS is first revealed in Section II. Section III discusses suitable optimization algorithms to showcase the optimal anchor placement layouts. These layouts are determined for scenarios with a different number of anchors in Section V, and are compared to the obtained CRLBs that are established in Section IV. Concluding remarks are given in Section VI.

II. ULTRASONIC INDOOR POSITIONING SYSTEM

The IPS considered in the anchor placement problem uses ultrasonic chirp signals to perform ToF ranging, as elaborated in previous work [11]. The speakers, acting as anchor nodes located at known positions $\mathbf{a}_j = [x_j, y_j, z_j]^T$, sequentially send a 30 ms chirp signal ranging from 25 kHz to 45 kHz. The mobile node, located at position $\mathbf{p} = [x, y, z]^T$, is equipped with a microphone and receives a portion of the chirp (1 ms) at a given synchronization interval. Depending on the distance between the microphone and corresponding speakers, a different part of the chirp will be received. Upon reception, a correlation, i.e., a pulse compression, is performed between

the received chirp part and the transmitted chirp. Given the planned synchronization, a time measurement and thus a ranging estimate can be made on the basis of the peak value of the correlation function. To better determine this peak value, a low-pass filter (LPF) is applied to the absolute value of the correlation function. Due to reverberation, it is possible that no unambiguously correct peak can be determined, which means that the estimate may give incorrect results. In addition to peak selection methods as described in [12], we here investigate the hypothesis that more redundancy can also be created when multiple distributed anchors are deployed, allowing for more accurate position estimates. To validate the latter, we focus for the ranging estimate on the maximum LPF value. After the ranging estimates between the anchors and mobile node, a least squares (LS) positioning algorithm is applied to estimate the 3D position.

In reality, there are limitations in terms of placing anchor nodes in a given room, which is the motivation of this work. To this end, this study investigates the (constrained) problem of finding an optimal placement of M anchors for the purpose of accurate positioning of a mobile device. The focus lies on achieving a high positioning accuracy over the whole coverage area, with the performance analyzed at the example of the ‘Techtile’ testbed environment, as described in [13]. To smoothly test different optimization techniques, this environment was simulated with the help of a realistic simulator which models reverberation and takes the directivity of nodes into account [10]. For practical reasons, it is assumed that the anchors (speakers) can only be attached to the two largest side walls and the ceiling of the $8\text{ m} \times 4\text{ m} \times 2.4\text{ m}$ room. The installation further requires that an anchor node has a 3 cm distance from a plane, while a mobile node is at least 5 cm away from a room plane.

III. ANCHOR LAYOUT OPTIMIZATION ALGORITHMS

An anchor placement solution can be found after an extensive search in which an optimization parameter is evaluated to yield positioning performance as close as possible to the CRLB, as mentioned in Section I. Besides extensive search algorithms, heuristic solutions, such as PSO could pave the way to an optimal solution wherein the craved computational resources remain limited compared to an extensive search. Other heuristic methods could possibly be applied, such as GAs [1] or gray wolf optimization (GWO) [9], yet in the scope of this work we focus on the PSO which features are specifically suited for the problem at hand.

A. Extensive Search Algorithm

An extensive search to find a global optimum is very effective since practically all possible placement combinations for anchor nodes are tested. Depending on the size of the room and the size of the mutual distance between the anchors to be tested, the number of possible combinations can quickly increase. Assume in total N potential anchor positions at the desired surfaces in a room, comprising the search space. M of these anchor positions will be used for the deployment of

anchors and thus positioning. In order to test all the combinations, $\binom{N}{M}$ simulations need to be performed. For example, if a set of 100 anchors is created in which all combinations of 6 anchors are tested, then 11.9×10^8 simulations must be performed and evaluated. Moreover, we want to test this not only for a selection of 6 anchors, but for $N \in \{4, 6, \dots\}$ anchors whereby a set of 100 anchor nodes to perform an extensive search itself remains limited to really find the best option. Omitting the number of combinations that all lie in the same plane and are therefore unable to provide good 3D positioning only reduces the total number of combinations to be tested by a fraction. The fact that this brute-force approach may have a very large search space and thus comes at a huge computational complexity and hence is not practical for all applications, urges other optimization methods to be developed.

B. Particle Swarm Optimization

Finding a global optimum often requires an extensive search and is thus difficult to obtain, a sub-optimal or local optimum solution derived from a heuristic solution is preferred to find solid anchor placement layout results. A best solution is usually out of the question, but there are several (sub-)optimal layouts where similar results can be obtained. The positioning accuracy will be substantially better compared to a random anchor placement, allowing to avoid time consuming extensive search algorithms. As a heuristic method, we propose to apply PSO due to its simplicity and fast convergence, in addition to the ability to handle a wide range of functions and constrained problems [14].

The PSO algorithm is inspired by the behaviour of birds or fish, which move in flocks or schools in order to avoid predators or find food. In this work, the PSO algorithm initializes a population, termed a swarm, of different candidate solutions/anchor placements of M anchor locations, as particles in the search space. To converge to an optimal solution, particles that are part of a given swarm update their relative positions iteratively in order to minimize a given cost function [14]. The movement of particle i is guided by their personal best position $\mathbf{p}_{\text{best},i}$ and global best position $\mathbf{g}_{\text{best},i}$ of the swarm. The personal best position of particle i are the M anchor positions, stacked as $\mathbf{x}_i = [\mathbf{a}_{1,i}^T, \dots, \mathbf{a}_{M,i}^T]^T$, that results in the lowest cost function value (i.e. Euclidean distance error variance) over the iterations given by iteration indices $t \in \{1, 2, \dots\}$. To determine the global best position, in addition to the best outcome of the past iterations, the best outcome of all the particles is also considered. The update performed between iterations is summarized as

$$\mathbf{v}_i^{t+1} = \omega \mathbf{v}_i^t + c_1 \mathbf{r}_1 (\mathbf{p}_{\text{best},i}^t - \mathbf{x}_i^t) + c_2 \mathbf{r}_2 (\mathbf{g}_{\text{best},i}^t - \mathbf{x}_i^t) \quad (1)$$

$$\mathbf{x}_i^{t+1} = \mathbf{x}_i^t + \mathbf{v}_i^{t+1} \quad (2)$$

where $\mathbf{v}_i = [\mathbf{v}_{i,1}^T, \dots, \mathbf{v}_{i,M}^T]^T$ represents the velocity vector of particle i which depends on the inertia weight ω representing a balance between local exploitation and global exploration, determining the partial influence that the previous velocity should have on the current movement. The coefficients c_1 and

c_2 are the cognitive and the social coefficients respectively, which are multiplied with the uniformly distributed random vectors \mathbf{r}_1 and \mathbf{r}_2 to maintain diversity in the swarm population [15]. The choice of hyperparameters ω , c_1 and c_2 needs to be determined based on a search approach for the specific application [15]. After the update in Eq. (2), some positions need to be reinforced again to remain within the search space, i.e, in our case, on certain room planes. Projections onto the nearest plane that is an element of the search space solve this problem. This also allows anchors to jump room planes instead of staying on their initialized plane.

IV. CRLB FOR TOF-BASED INDOOR POSITIONING

The CRLB is used as a reference to compare the performance obtained from the PSO algorithm over iterations and for different numbers and positions of anchors. Based on [16], we assume that the range measurements obtained from the correlation function discussed in Section II can be modeled as the true distances $d_j(\mathbf{p})$ between mobile node and speakers $j \in \{1, \dots, M\}$, corrupted with additive white gaussian noise (AWGN) noise [16]. This yields a range measurement model according to

$$r_j = \|\mathbf{p} - \mathbf{a}_j\| + n_j = d_j(\mathbf{p}) + n_j \quad (3)$$

where n_j is the range measurement noise and $\|\cdot\|$ denotes the Euclidean norm. The measurements for different speakers are assumed to be statistically independent, with n_j modeled as zero mean Gaussian noise [16] with variance $\sigma_{r,j}^2$.

The CRLB gives a lower bound for the variance of any unbiased estimator. It is calculated using the inverse of the Fisher information matrix (FIM) $\mathbf{J}(\mathbf{p})$ as [17]

$$\mathbb{E}[(\hat{\mathbf{p}} - \mathbf{p})(\hat{\mathbf{p}} - \mathbf{p})^T] \succeq \mathbf{J}(\mathbf{p})^{-1} \quad (4)$$

with the entry of row m and column n of the FIM defined as the partial derivative of the log-likelihood function $\ln f(\mathbf{r}|\mathbf{p})$ of all range measurements $\mathbf{r} = [r_1, \dots, r_J]^T$.

$$[\mathbf{J}(\mathbf{p})]_{mn} = -\mathbb{E}\left[\frac{\partial^2 \ln f(\mathbf{r}|\mathbf{p})}{\partial[\mathbf{p}]_m \partial[\mathbf{p}]_n}\right] \quad (5)$$

Assuming independent measurements to all anchors, the measurement likelihood function factorizes as $f(\mathbf{r}|\mathbf{p}) = \prod_{j=1}^J f(r_j|\mathbf{p})$, with the j th anchors likelihood $f(r_j|\mathbf{p})$ being Gaussian due to the model from (3). The CRLB allows to obtain a reference for performance comparison of the PSO algorithm described in Section III. Following the derivation from [18] one obtains

$$[\mathbf{J}(\mathbf{p})]_{mn} = \sum_{j=1}^J \frac{1}{\sigma_{r,j}^2} \frac{[\mathbf{p} - \mathbf{a}_j]_m}{\|\mathbf{p} - \mathbf{a}_j\|} \frac{[\mathbf{p} - \mathbf{a}_j]_n}{\|\mathbf{p} - \mathbf{a}_j\|}. \quad (6)$$

The position error bound (PEB) for a mobile node at position \mathbf{p} is then defined as the trace of the position CRLB

$$\text{PEB}(\mathbf{p}) = \text{tr}[\mathbf{J}(\mathbf{p})^{-1}]. \quad (7)$$

V. SIMULATION RESULTS

This section discusses the simulation results of two investigated scenarios: the optimal placement of $M = 4$ anchors showing the performance over PSO iterations, and the performance comparison of optimal anchor placements for multiple distributed anchors exploring $M = \{4, 6, 8, 10\}$. The CRLB outlined in Section IV is used as performance reference.

A. Optimal Anchor Placement

The impact of the anchor placement layout is examined by comparing a non-optimized and optimized scenario. In both cases, 4 anchors are used to perform 3D indoor positioning for 270 mobile node positions, which are evenly distributed over the room on a regular grid. The spacing along the x , y and z axes of the mobile node locations is 98.8 cm, 78.0 cm and 57.5 cm respectively. The anchors are placed in the room as described in Section II and take into account the stated limitations. The sampling frequency of the signals received by each mobile nodes' microphone is chosen to be 192 kHz to meet realistic hardware specifications for audio sampling. For the microphones, an omni-directional directivity is assumed, while the speakers apply a cardioid pattern to exhibit a realistic model. As an additional assumption, the directivity vector of the speakers always points towards the centroid of the room. The signal-to-noise ratio (SNR) is defined for the closest mobile node to a specific anchor and is chosen as 30 dB. An equivalent amount of noise is then added to the received signals of the other mobile nodes from that specific anchor. This results in different noise standard deviation values for the different anchors since the distances to the closest mobile nodes are similar but not the same. For the obtained optimal anchor placement discussed in this section, the noise standard deviation for the 4 different anchors varies between $\sigma_n = 0.0016$ and $\sigma_n = 0.0079$. Due to the fact that the positions of the anchors change over iterations, these noise values will also change.

To perform the search for optimum anchor placement in terms of a high positioning accuracy at all investigated mobile node positions, the PSO algorithm from Section III is applied. At each iteration i each particle \mathbf{x}_i contains all positions of the 4 anchors. The swarm, in this case, counts 15 particles. The initialization phase creates these randomly placed particles, taking into account the constraints and assumptions. In the considered application, anchors can only be installed on the two largest walls and the ceiling. The anchors are distributed based on surface ratios with more anchors placed on larger surfaces. In the case of 4 anchors, this means that both walls get 1 anchor, and the ceiling the remaining 2. In all cases, the directivity is pointing towards the room centroid. During the PSO iterations, the simulations are performed to obtain a positioning improvement based on a proposed optimization metric/cost function. The variance of the Euclidean distance error of all position estimates is used as a metric, since the smallest possible error is desired over the entire space. The smaller the variance, the steeper the slope of the resulting cumulative distribution function (CDF) or generally the

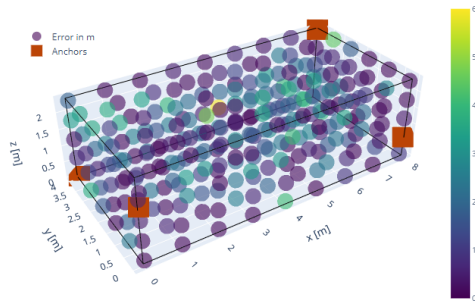


Figure 1: Euclidean distance errors for the non-optimized 4 anchor placement.

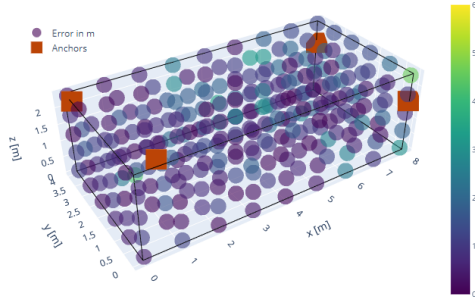


Figure 2: Euclidean distance errors for the optimized 4 anchor placement.

smaller the chance of large observed outliers. When updating the anchor positions between iterations, it may happen that the anchors are no longer placed within the search space (on the certain surfaces). This is again enforced through projections onto the nearest planes as discussed in Section III. Subsequently, the directivity vector is adjusted. After several iterations, the improvement per iteration will drop below an arbitrary threshold, meeting the stopping criteria

For the non-optimized scenario, the anchors are placed at the wall and ceiling corners of the room, as illustrated with the orange squares in Fig. 1, so that when the neighboring anchors are fictitiously connected together with a line, the envelope curve encompasses the room. Intuitively, it seems that this should give better positioning accuracy results since the mobile nodes are within the envelope of the anchors.

The 3D Euclidean distance errors between the real and estimated positions and the anchor placements for the non-optimized and optimized scenarios are shown in Fig. 1 and Fig. 2. The standard deviation values for the non-optimized and optimized scenarios are respectively 1.362 m and 0.811 m. It can be seen that in general the accuracy of almost all position estimates increased after optimization, at the expense of decreased accuracy for a few positions. Most notably, large outliers are eliminated. An optimal scenario for all positions, which strongly depends on the application and optimization parameter, is not possible but it can be aspired to be achieved.

The accompanying CDF curves, shown in Fig. 3, indicate the relationship between x , y and z errors, in addition to the Euclidean distance error, between the optimized and non-optimized setup. During the optimization process, the accuracy

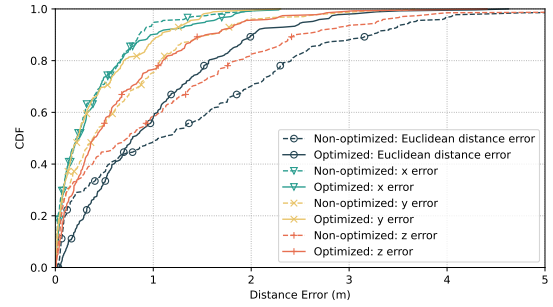


Figure 3: Comparison between the Euclidean 3D distance, x , y and z error values obtained by the optimized and non-optimized IPS.

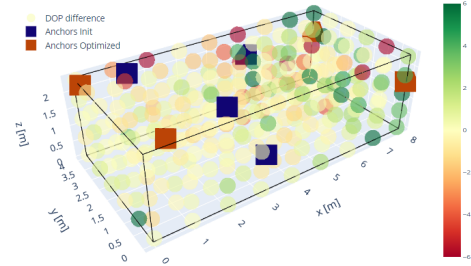


Figure 4: DOP difference between the initialized and optimized 4 anchors scenario.

along the x -direction drops slightly, when looking at the P95 value, to noticeably improve both the y and z accuracy and thus overall Euclidean distance accuracy. The evolution of accuracy improvement over PSO iterations can also be shown by the difference in obtained DOP values. The DOP provides an indication of how well the anchor geometry can determine a mobile node's position. After performing $R = 500$ realizations of the specific initialization and optimal solution scenario, the standard deviation for the Euclidean distance σ and ranging σ_r at each position can be determined. σ_r at a certain mobile node position in this case is the average of the standard deviations $\sigma_{r,j}$ obtained from each of the 4 anchors. The DOP for each position is defined as $DOP^p = \sigma^p / \sigma_r^p$. Fig 4 shows the DOP improvement between the initialized and optimal scenario at each position as $DOP_{init}^p - DOP_{opt}^p$. Concluded from this figure, the DOP across all mobile node positions improves at most locations and deteriorates at few. On average, the DOP over all positions for these scenarios improved from 2.52 to 1.74.

To investigate the performance of the PSO algorithm, the CRLB described in Section IV is compared to the RMSE of the position estimates for $R = 500$ realizations. For the numerical evaluation of the CRLB, the distance estimates were used to obtain the necessary range standard deviation for each anchor, which were in the range of $\sigma_r \approx 0.03 - 0.045$ m. It should be noted that after removing outliers occurring at some positions, the range measurements for each anchor were reasonably well approximated as Gaussian distributed. Fig. 5 shows the CDFs of the PEB and the RMSE for iterations $t = \{1, 20, 40\}$ for $M = 4$ anchors. While the CDF of the PEB shows a generally

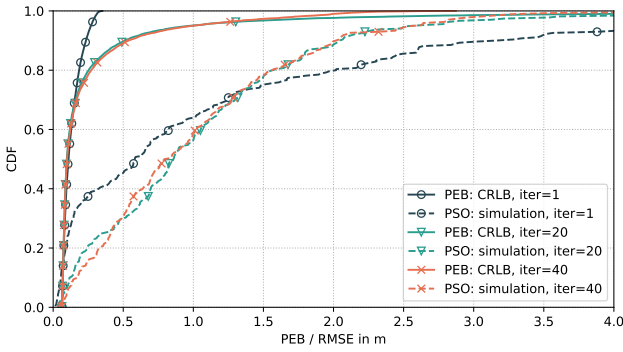


Figure 5: Comparison between CDFs of the root-mean-square error (RMSE) and the PEB (via CRLB, neglecting outliers) obtained for the PSO iterations $t = \{1, 20, 40\}$ for 4 anchors.

lower error over all candidate positions for the first iteration, the PSO algorithm results show an improvement, especially above the P95 value. Most notably, for both the PEB as well as the RMSE curves, the only change from iteration 20 to 40 is the reduction of outliers, i.e., the maximum value of 1 is reached at lower error values. Comparing the first iteration, the RMSE initially follows the PEB until deviating, which can be explained by the fact that even though the range estimates are approximately Gaussian, outliers in the PSO simulation remain that are most likely attributable to overlapping propagation paths. This overlap introduces outliers that are on the one hand not captured in the bounds, but also not easy to include. Therefore, the range measurement model used for the CRLB determination is too limited. Nonetheless, the PSO simulation shows that the proposed optimization scheme is well suited to use for realistic scenarios, where a CRLB based analysis based on the given range measurement model could give over optimistic results and worse performance, especially for difficult measurement models.

Fig 6 shows the distribution of the PEB in 3D alongside the anchor positions per iteration. While initially showing a “favorable” anchor geometry for iteration 1, the anchors converge to being positioned close to a plane, which results in a larger error perpendicular to that plane for agent positions on the plane. While non-optimal from a CRLB point of view, the CDF comparison derived from the PSO simulations has shown that it is nonetheless well suited for that specific environment.

Overall it can be seen that the anchor placement layout can

play a major role in the accuracy of an IPS. Another room or the same room with more or fewer mobile nodes may prefer a different optimal anchor placement layout, depending on the optimization parameter choice.

B. Multiple Anchors

Besides the anchor placement, the number of distributed anchors in the room has an influence on the accuracy and reliability of the IPS. To investigate this influence, situations are simulated with 4, 6, 8 and 10 anchors. An optimal anchor placement was first determined for each situation, as shown in Fig. 7 using PSO to allow for a fair comparison between the best configurations. The standard deviation σ , mean μ and P95 values of the common Euclidean distance error are derived from simulation and summarised in Table I.

Anchors	4	6	8	10
σ (m)	0.803	0.691	0.587	0.563
μ (m)	0.995	0.913	0.797	0.773
P95 (m)	2.629	2.272	1.986	1.876

Table I: Comparison between σ , μ and P95 values of the Euclidean distance errors for the 4, 6, 8 and 10 optimal anchor placement scenarios, derived from simulations.

As expected, the standard deviation σ , mean μ and especially P95 values decrease as the number of anchors increases. The CDF functions of the Euclidean distance error of the 3D position estimates alongside the PEB results are shown in Fig. 8. Both show an accuracy improvement when using multiple anchors. The achievable simulated positioning accuracy for this room shows minimal difference between 8 and 10 anchor nodes. Saturation of the accuracy values is observed for 8 anchors and no major improvement is expected with the addition of even more anchors. In more complex rooms with locations NLoS condition and possibly more reverberation, this saturation point is expected to be at a higher number.

While the use of multiple anchor nodes is desirable in terms of achievable accuracy, it is detrimental to the complexity, installation and update rate. The latter can be avoided by coding or by using frequency-division multiplexing (FDM) instead of time-division multiplexing (TDM) to avoid interference between anchors. If non-optimized anchor placements are used, the deployment of multiple anchors can ensure that

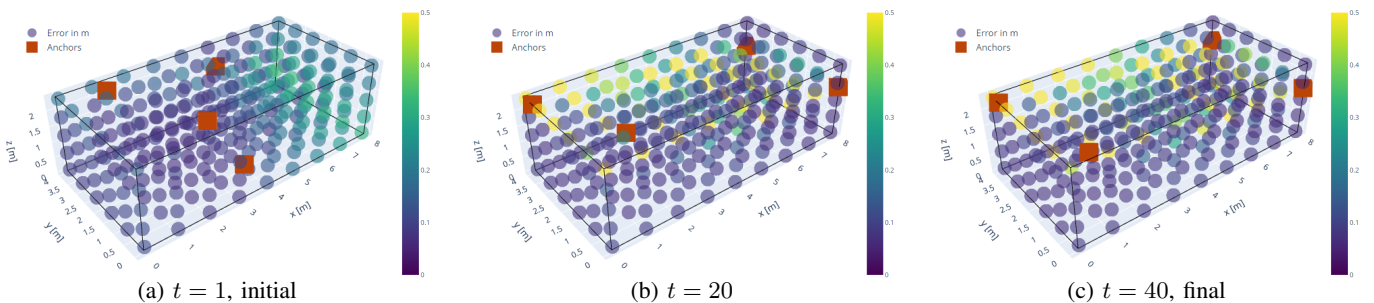


Figure 6: Evolution of the PEB based on the CRLB for the PSO algorithm iterations $t = \{1, 20, 40\}$ for 4 anchors.

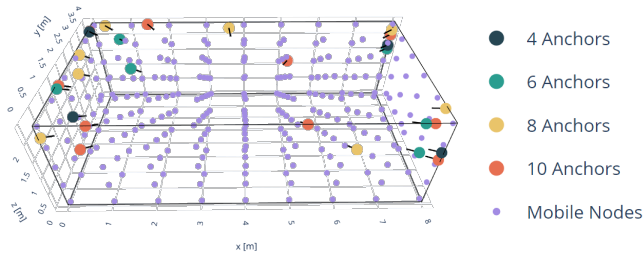


Figure 7: Obtained anchor placement layout after PSO

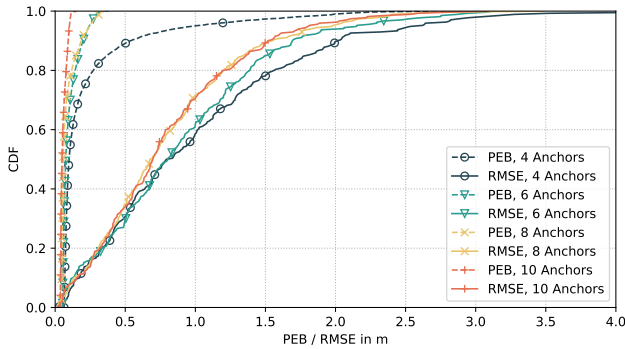


Figure 8: Comparison between CDFs of the simulated Euclidean 3D distance and PEB (via CRLB) obtained by the 4, 6, 8 and 10 optimal anchor placement scenarios.

a more optimal anchor combination, which is part of the non-optimized set, can be used to increase the precision at a specific location. However, this requires selection algorithms to choose the right set of anchors at a certain mobile node location. The anchor placement has a bigger impact on the precision and reliability than the amount of anchors used within an IPS employing the minimum amount of anchors necessary to perform unambiguous positioning.

VI. CONCLUSION

A PSO method to obtain an optimal anchor placement layout for a 3D IPS was presented. Based on simulations performed with this algorithm and a CRLB analysis, it can be concluded that a more optimal anchor placement layout for the IPS results in a desired increase in positioning accuracy and reliability within the entire room. There is even more to gain in having multiple anchors at distributed locations, taking into account an accuracy saturation at a certain number of anchors. An improvement of 30% and 29% on respectively the standard deviation and the P95 value is observed if 10 instead of 4 optimally placed anchors are applied. The improvements are expected to be even more extreme in advanced complex rooms with supplementary reverberation and NLoS effects. In addition, the cost function also plays an important role in developing the optimal anchor layout, with the actual choice of cost function being application dependent. Note that it is easy to adjust the cost function of the optimization method. The positioning system with optimal anchor placements will be validated via measurements in future work.

ACKNOWLEDGMENT

This work was supported by the Research Foundation-Flanders (FWO) under Grant GOD3819N. This work has been partly supported by the European Union's Horizon 2020 research and innovation programme REINDEER project under grant agreement No. 101013425.

REFERENCES

- [1] S. Haigh, J. Kulon, A. Partlow, and C. Gibson, "Comparison of objectives in multiobjective optimization of ultrasonic positioning anchor placement," *IEEE Transactions on Instrumentation and Measurement*, vol. 71, pp. 1–12, 2022.
- [2] T. Qiao and H. Liu, "Incremental anchor layout for indoor positioning," in *2017 IEEE International Conference on Communications (ICC)*, 2017, pp. 1–6.
- [3] N. Lasla, M. Younis, A. Ouadjaout, and N. Badache, "On optimal anchor placement for efficient area-based localization in wireless networks," in *2015 IEEE International Conference on Communications (ICC)*, 2015, pp. 3257–3262.
- [4] A. Cheriet, A. Bachir, N. Lasla, and M. Abdallah, "On optimal anchor placement for area-based localization in wireless sensor networks," *IET Wireless Sensor Systems*, vol. 11, Apr. 2021.
- [5] R. Sharma and V. Badarla, "Geometrical optimization of a novel beacon placement strategy for 3D indoor localization," in *2018 IEEE International Conference on Advanced Networks and Telecommunications Systems (ANTS)*, 2018, pp. 1–6.
- [6] M. M. Faraji, S. B. Shouraki, E. Iranmehr, and B. Linares-Barranco, "Sound source localization in wide-range outdoor environment using distributed sensor network," *IEEE Sensors Journal*, vol. 20, no. 4, pp. 2234–2246, 2020.
- [7] K. Frampton, "Acoustic self-localization in a distributed sensor network," *IEEE Sensors Journal*, vol. 6, no. 1, pp. 166–172, 2006.
- [8] A. El Assaf, S. Zaidi, S. Affes, and N. Kandil, "Optimal anchors placement strategy for super accurate nodes localization in anisotropic wireless sensor networks," in *2016 Intl. Wireless Communications and Mobile Computing Conference (IWCMC)*, 2016, pp. 25–30.
- [9] T. Çavdar, F. B. Günay, N. Ebrahimpour, and M. T. Kakız, "An optimal anchor placement method for localization in large-scale wireless sensor networks," *Intelligent Automation & Soft Computing*, vol. 31, no. 2, pp. 1197–1222, 2022.
- [10] D. Delabie, C. Buyle, B. Cox, L. V. der Perre, and L. D. Strycker, "An acoustic simulation framework to support indoor positioning and data driven signal processing assessments," in *2023 IEEE European Signal Processing Conference (EUSIPCO)*, 2023. arXiv: 2305.02715.
- [11] B. Cox, C. Buyle, D. Delabie, L. De Strycker, and L. Van der Perre, "Positioning energy-neutral devices: technological status and hybrid RF-acoustic experiments," *Future Internet*, vol. 14, no. 5, 2022.
- [12] B. Cox, C. Buyle, L. Van der Perre, and L. De Strycker, "Towards centimetre accurate and low-power, hybrid radio-acoustic 3D indoor positioning: an experimental journey," in *2021 IEEE Indoor Positioning and Indoor Navigation (IPIN)*, CEUR Workshop, 2021.
- [13] D. Delabie, B. Cox, L. De Strycker, and L. Van der Perre, "Techtile: A flexible testbed for distributed acoustic indoor positioning and sensing," in *IEEE Sensors Applications Symposium (SAS)*, 2022.
- [14] A. Gad, "Particle swarm optimization algorithm and its applications: A systematic review," *Archives of Computational Methods in Engineering*, vol. 29, Apr. 2022.
- [15] D. Freitas, L. G. Lopes, and F. Morgado-Dias, "Particle swarm optimisation: A historical review up to the current developments," *Entropy*, vol. 22, no. 3, 2020.
- [16] B. Cox, L. Van der Perre, S. Wielandt, G. Ottoy, and L. De Strycker, "High precision hybrid RF and ultrasonic chirp-based ranging for low-power IoT nodes," *Eurasip Journal On Wireless Communications And Networking*, no. 1, pp. 1–24, 2020.
- [17] S. M. Kay, *Fundamentals of Statistical Signal Processing, Vol. I: Estimation Theory*. Signal Processing. Upper Saddle River, NJ: Prentice Hall, 1993.
- [18] I. Guvenc and C.-C. Chong, "A survey on TOA based wireless localization and NLOS mitigation techniques," *IEEE Communications Surveys & Tutorials*, vol. 11, no. 3, pp. 107–124, 2009.